# Investigation of the Melting Behavior of Poly(aryl ether ketones) by Simultaneous Measurements of SAXS and WAXS Employing Synchrotron Radiation

**K.-N. Krüger and H. G. Zachmann***

*Institut für Technische und Makromolekulare Chemie, University of Hamburg, Bundesstrasse 45, D20146 Hamburg, Germany*

*Received October 28, 1992; Revised Manuscript Received June 7, 1993*

ABSTRACT: Samples of poly(ether ether ketone) (PEEK), poly(ether ether ketone ketone) (PEEKK), and poly(ether ketone ether ketone ketone) (PEKEKK) were crystallized at different temperatures by stepwise cooling from the melt to obtain samples which show multiple melting peaks in a calorimetric investigation. The melting behavior of these materials was investigated by wide-angle X-ray scattering (WAXS) and small-angle X-ray scattering (SAXS) employing synchrotron radiation and by differential scanning calorimetry (DSC). The change of the degree of crystallinity, of the small-angle X-ray scattering power $Q$, and of the long period was determined as a function of temperature during heating. It was concluded that the additional melting peaks are caused by melting of some thin crystals within lamellar stacks and not by melting of complete lamellar stacks. In addition, some partial melting of crystals starting from their surfaces seems to take place.

## Introduction

The occurrence of double melting peaks in the differential scanning calorimetry (DSC) diagrams during heating of polymers is a long-known phenomenon. Though some attempts have been made to explain the presence of these double melting peaks by assuming different kinds of crystals such as folded chain crystals, bundle-like crystals, and extended chain crystals,[1,2] in most cases it has been shown that double melting peaks either are a consequence of melting and recrystallization during heating[3-7] or are due to the existence of two populations of crystal lamellae with different thicknesses.[8-12]

There still exists the question of whether the crystals with the higher melting point are all formed by recrystallization during heating or whether they are, at least in part, present from the beginning of the experiment. For poly(ethylene terephthalate) (PET) it has been clearly demonstrated[13] that, for example, after crystallization at 140 °C, all crystals had a melting point of less than 247 °C, which is 21 °C below that which is usually found. When such a material is heated in a DSC experiment, crystals with the equilibrium melting point are only obtained by recrystallization at higher temperatures. In contrast, there exists some evidence that crystals with the high melting point are formed immediately during crystallization in the case of PEEK.[9]

In recent investigations it was shown that it is possible to obtain more than two melting peaks by subsequent crystallization at different temperatures. Thus up to ten melting peaks were obtained in poly(ether ether ketone) (PEEK)[14-16] and up to four in poly(ether ether ketone ketone) (PEEKK).[11]

In addition to the DSC measurements, there also exist some investigations of melting and recrystallization by means of small-angle X-ray scattering (SAXS) and wide-angle X-ray scattering (WAXS) employing synchrotron radiation. It was found for PET and poly(ethylene naphthalene-2,6-dicarboxylate) (PEN) that partial melting and recrystallization take place within the lamellar stacks without changing the fraction of spherulitically crystallized material.[17-19] In a very interesting investigation on PEEK, Hsiao et al.[10] have shown that the first of two melting peaks observed in the previously isothermally crystallized material corresponds to a stepwise increase of the long period. This was explained by assuming that some thinner lamellar crystals within the lamellar stacks are melting and that crystals with the higher melting point are present already at the beginning of the heating experiment. Quite recently, the melting of thinner crystal lamellae during heating of PEEK was directly observed by electron microscopy.[12]

In the present work we have performed melting investigations on PEEK, PEEKK, and poly(ether ketone ether ketone ketone) (PEKEKK) by means of SAXS and WAXS employing synchrotron radiation. The samples were crystallized subsequently at different temperatures to obtain DSC curves showing up to five melting peaks. The changes of the long period $L$ and the scattering power $Q$ obtained by SAXS are compared to the changes of the degree of crystallinity obtained by WAXS and DSC.

**Table I. Annealing Temperatures $T_{cl}$ (°C) for the PAEK Samples[a]**

| sample | $T_{c1}$ | $T_{c2}$ | $T_{c3}$ | $T_{c4}$ | $T_{c5}$ | $T_{c6}$ |
|---|---|---|---|---|---|---|
| PEEK A | 302 | 272 | | | | |
| PEEK B | 302 | 287 | 272 | 257 | 242 | 227 |
| PEEKK | 347 | 317 | 287 | | | |
| PEKEKK | 352 | 322 | 292 | | | |

[a] At each temperature the samples were annealed for 1 h.

## Experimental Section

The investigations were performed on PEEK (Stabar) obtained as an amorphous film from ICI, on PEEKK (Hostatec) obtained as a powder from Hoechst, and on PEKEKK (Ultrapek) received as granulates from BASF.

Amorphous films were prepared by melt pressing and quenching. Circular samples with a diameter of 2 cm and a thickness of approximately 250 μm were melted on a Linkham hot stage for 10 min at 380 °C in the case of PEEK and at 420 °C in the case of PEEKK and PEKEKK and then cooled successively to different crystallization temperatures at a rate of 99 °C/min. They were kept at each temperature for 1 h. The different temperatures which were used are shown in Table I.

The calorimetric measurements were performed on a DuPont 910 DSC, using a heating rate of 5 °C/min.

The SAXS and WAXS experiments were performed at the polymer beam line at HASYLAB (DESY, Hamburg). A double-focusing camera was used, which is described in detail in earlier publications.[17,20] To measure the WAXS and SAXS simultaneously, the WAXS is transformed by a fluorescence screen into

0024-9297/93/2226-5202$04.00/0 

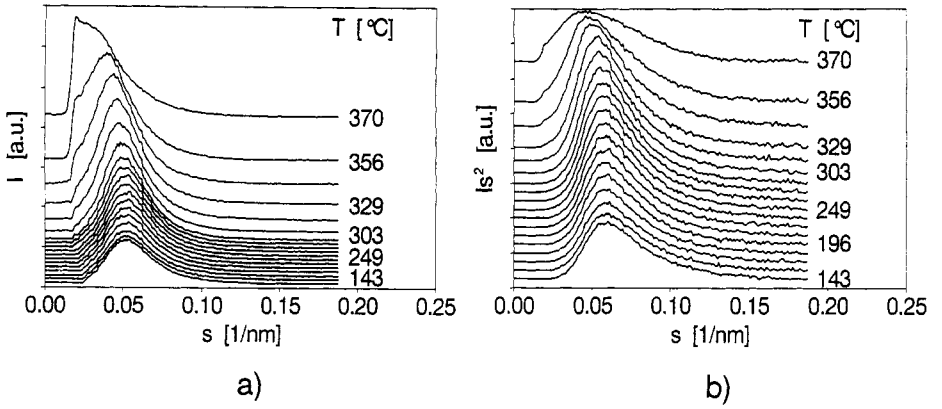


**Figure 1.** Change of small-angle X-ray scattering during heating (5 °C/min) of the PEEKK sample as a function of the scattering vector $s$: (a) scattering intensity $I$; (b) Lorentz-corrected intensity $Is^2$.

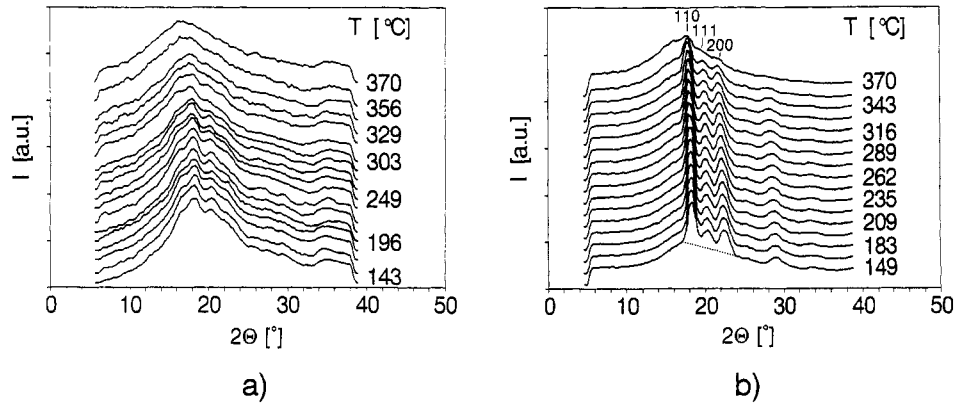


**Figure 2.** Change of the wide-angle X-ray scattering during heating (5 °C/min) of the PEEKK sample. Scattering intensity $I$ as a function of the scattering vector $s$: (a) from simultaneous SAXS/WAXS measurements; (b) from separate measurements by a linear position sensitive Gabriel detector.

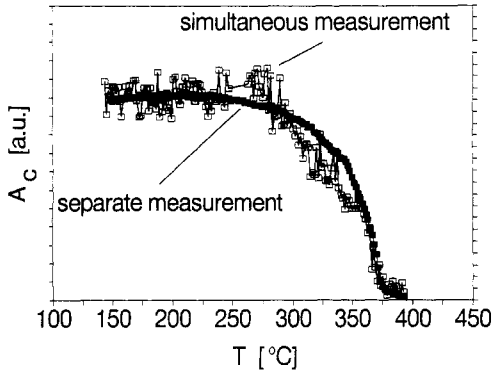


**Figure 3.** Integrated WAXS crystal reflection intensity as a function of temperature for the PEEKK sample as obtained in the simultaneous measurements (□) and as obtained in the separate measurements (■).

visible light and is reflected through an angle of 90° by a mirror onto a vidicon.[19] The SAXS passes through a hole in the screen and a hole in the mirror to a one-dimensional Gabriel counter. In addition to the simultaneous measurements, the WAXS was separately measured by means of a one-dimensional Gabriel detector. The background scattering obtained when no sample was present in the beam was subtracted from all measured curves after proper correction with respect to absorption.[17] To take into account the change of the intensity of the primary beam during the measurement, the scattering intensity was divided by the intensity of the primary beam, as measured by an ionization chamber in relative units.

## Results

Figure 1a shows the SAXS curves obtained during heating at 5 °C/min of PEEKK which was first molten at 420 °C for 10 min and then, during cooling, successively crystallized at 355, 325, and 295 °C. One can clearly recognize a peak which is shifted to smaller angles with increasing temperature. Figure 1b shows the corresponding Lorentz-corrected curve of the SAXS where the intensity $I$ is multiplied by $s^2$ with $s = (2/\lambda)\sin(\theta/2)$, $\theta$ being the scattering angle. Figure 2a shows the WAXS curves which were measured simultaneously with the SAXS patterns in Figure 1. One can recognize some broad crystal reflections at low temperatures which gradually disappear with increasing temperature. The angular resolution in this experiment is very poor due to broadening in the fluorescence screen and the optical imaging process. A much better resolution is obtained if the WAXS is directly measured in a different experiment using a one-dimensional Gabriel detector. The corresponding curves are shown in Figure 2b.

For the evaluation of the WAXS curves, an amorphous halo was subtracted by connecting the scattering intensity at $2\theta = 17.2°$ and $2\theta = 24.1°$ by a straight line, as indicated for the bottom curve in Figure 2b by the dotted line. The shape of this line approximately corresponds to the shape of the curve obtained for the completely molten material. The area under the three crystal reflections (110, 111, and 200) was determined as a function of temperature. Figure 3 shows the results from the simultaneous measurements in which the fluorescence screen, the mirror, and the vidicon were used compared to those in which the linear Gabriel detector was directly applied. It is evident that the main features of the curves are the same. In particular, the melting points, where the areas under the crystal reflections become zero, coincide for both measurements. This proves that the temperatures measured during the two different experiments are in agreement. However, the scattering of the data obtained by the indirect

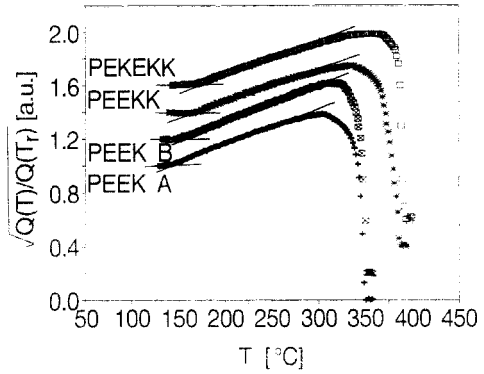


**Figure 4.** Square root of the scattering power $Q$ as a function of temperature for all four samples investigated in this work.

simultaneous measurements is much larger than the scattering of the data directly measured by the linear detector. The same turned out to be true for the other samples. Therefore, in the following, only the curves directly measured by the linear detector in a separate experiment will be presented in the figures.

For the evaluation of the SAXS experiment the scattering power $Q$ was determined. This quantity is defined as the intensity integrated over all scattering angles normalized with respect to the intensity of the primary beam, the volume of the sample, and the scattering power of a single electron. Because we were only interested in the change of $Q$, this normalization was not performed. Only the relative change of the intensity of the primary beam during the measurement was taken into account as described in the Experimental Section. As has been shown in previous publications[17,21-23]

$$Q = x_S x_L x_{cL}(1 - x_{cL})(\Delta\rho)^2 \quad (1)$$

where $x_S$ is the volume fraction filled with spherulites, $x_L$ is the volume fraction which has been transformed into lamellar stacks, $x_{cL}$ is the crystallinity within the spherulite, and $\Delta\rho$ is the difference between the densities of the crystalline and amorphous regions. If the sample is completely filled by spherulites, as is the case in this investigation, $x_S$ and $x_L$ are equal to 1.

With increasing temperature, $\Delta\rho$ increases due to the different thermal expansions of the crystals and the amorphous regions.[17] Because $\Delta\rho$ increases with increasing temperature, $Q$ should increase, according to eq 1, in proportion to the square of the temperature as long as $x_{cL}$ stays constant. Therefore we have plotted the square root of $Q(T)/Q(T_r)$ as a function of temperature $T$. $T_r$ is a reference temperature at which the measurement was started. This temperature was 140 °C for PEEK A and PEEK B and 150 °C for PEEKK and PEKEKK. The resulting curves are presented in Figure 4. By definition, each curve starts at the value 1. However, for clarity the curves for the samples PEEK B, PEEKK, and PEKEKK were shifted on the ordinate by 0.2, 0.4, and 0.6 units, respectively.

With increasing temperature, first a change in the slope of each curve is observed which can be attributed to the glass transition.[17,24] The glass transition temperatures $T_g$ obtained in this way are listed in Table II together with the glass transition temperatures reported in the literature.[25-27] The values we have found are somewhat larger than those reported in the literature, which may be due to the fact that our samples were crystalline. It is well known that crystallization may considerably increase the value of the glass transition temperature.[28]

Above $T_g$ (146, 150, 166, and 171 °C for PEEK A, PEEK B, PEEKK, and PEKEKK, respectively), over a temperature range of about 100 °C, a linear increase of $Q(T)/Q(T_r)$ is found. As expected, no indication of melting is found by DSC and WAXS in this temperature range. Therefore, the linear increase is attributed to a change of $\Delta\rho$.

**Table II. Glass Transition Temperatures $T_g$, Melting Temperatures $T_m$, and Differences in the Thermal Expansion Coefficients $\Delta\alpha$ As Obtained from Figure 4**

| sample | $T_g$ (°C) this work | $T_g$ (°C) lit. | $T_m$ (°C) this work | $T_m$ (°C) lit. | $\Delta\alpha$ [g/(cm³ K)] above $T_g$ |
|---|---|---|---|---|---|
| PEEK A | 146 | 144[25] | 350 | 335[25] | 0.019 |
| PEEK B | 150 | 144[25] | 351 | 335[25] | 0.019 |
| PEEKK | 166 | 160[26] | 388 | 365[26] | 0.019 |
| PEKEKK | 171 | 170[27] | 392 | 381[27] | 0.017 |

Finally, at higher temperatures, a deviation from the straight line to lower values is observed, which is explained by the decrease of crystallinity due to melting. The value at which $Q$ becomes zero is the melting point $T_m$ of the material. The values obtained for $T_m$ are listed in Table II, together with those known from the literature.[25-27]

To use the change of $Q$ as a measure for the variation of crystallinity, one has to eliminate the effect of thermal expansion. For this purpose, we have calculated the difference of the thermal expansion coefficients of the crystals and the amorphous regions, $\Delta\alpha$, as described in the following:[17] We have

$$\Delta\rho = \Delta\rho_0 + (T - T_r)\Delta\alpha \quad (2)$$

where $\Delta\rho_0$ is the density difference between crystals and amorphous regions at the reference temperature $T_r$. $\Delta\rho$ is the density difference at the temperature $T$, and $\Delta\alpha$ the difference of the thermal expansion coefficients of the crystals and the amorphous regions. The thermal expansion coefficient is defined as the change of density per kelvin. By inserting this expression for $\Delta\rho$ in eq 1, we obtain

$$\left[\frac{Q(T)}{Q(T_r)}\right]^{1/2} = 1 + \frac{\Delta\alpha}{\Delta\rho_0}(T - T_r) \quad (3)$$

Thus, the slopes of the lines in Figure 4 are given by $\Delta\alpha/\Delta\rho_0$. As one knows $\Delta\rho_0$, one can calculate $\Delta\alpha$ from the slopes. The results are shown in Table II.

Next, by using these values of $\Delta\alpha$, one can calculate the density difference $\Delta\rho$ as a function of $T$ by means of eq 2. From this it is possible to calculate a corrected scattering power

$$Q_{cor} = Q/\Delta\rho^2 \quad (4)$$

Figure 5 shows the corrected scattering power $Q_{cor}$, the long period $L$, the area under the crystal reflections $A_c$, and the DSC curves of the PEEKK sample from Figures 1 and 2. In addition, the derivative of $A_c$ with respect to $T$ is given for a better comparison with the DSC curve. Before differentiating $A_c$, we smoothed the curve by using a cubic spline function. The values of $Q_{cor}$ were obtained from the curves of Figure 1b after integration in the range from $s = 0$ to $s = 0.17$ nm$^{-1}$. For the determination of the long period, the SAXS curves were smoothed by successive averaging over three neighboring measured points. The curve representing $A_c$ is the same as $A_c$ from the separate experiment in Figure 3. Four melting peaks can be observed in the DSC diagram which are in good agreement with corresponding melting peaks in the $dA_c/dT$ curve. In the range where melting takes place, an increase of the long period is observed. The two last melting peaks are correlated with stepwise increases of $L$. However, there also exist regions in which $L$ does not change during

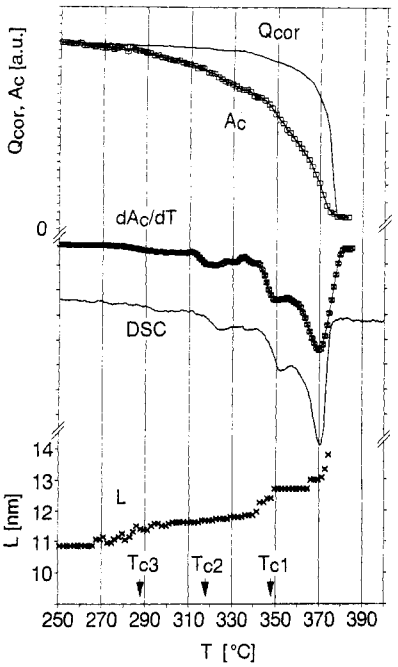


**Figure 5.** Corrected SAXS power $Q_{cor}$, integral intensity of the crystal reflections $A_c$, $A_c$ differentiated with respect to $T$, and long period $L$ as a function of temperature during heating (5 °C/min) of the PEEKK sample. In addition, the DSC curve is also presented. The annealing temperatures of previous crystallization (see Table I) are indicated by the arrows.

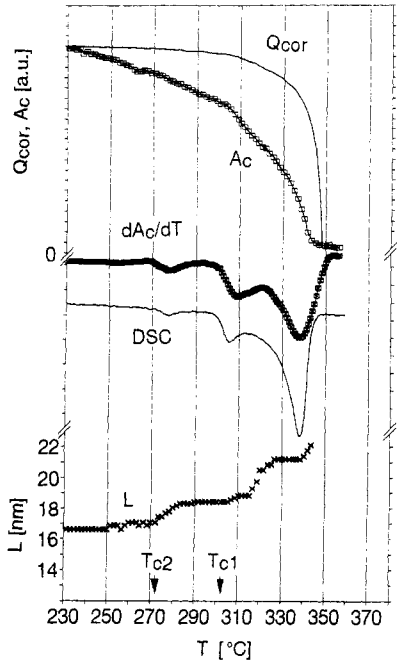


**Figure 6.** Corrected SAXS power $Q_{cor}$, integral intensity of the crystal reflections $A_c$, $A_c$ differentiated with respect to $T$, and long period $L$ as a function of temperature during heating (5 °C/min) of the PEEK A sample. In addition, the DSC curve is also presented. The annealing temperatures of previous crystallization (see Table I) are indicated by the arrows.

melting, for example, in the temperature range 350–365 °C. The gradual melting is also reflected in the curve $A_c$ representing the change of the integrated intensity of the crystal reflection. As the curve $A_c$ corresponds to the integrated DSC curve, it shows less significant features than the DSC curve. Nevertheless, at the two largest peaks of the DSC curve, the slope of the $A_c$ curve is also largest. In the temperature range up to 340 °C, the relative change of $Q_{cor}$ is smaller than that of $A_c$. This can be explained if one considers that, according to eq 1, $Q_{cor}$ is proportional

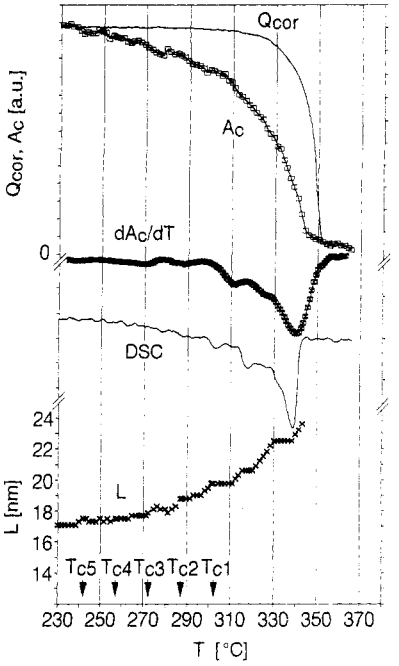


**Figure 7.** Corrected SAXS power $Q_{cor}$, integral intensity of the crystal reflections $A_c$, $A_c$ differentiated with respect to $T$, and long period $L$ as a function of temperature during heating (5 °C/min) of the PEEK B sample. In addition, the DSC curve is also presented. The annealing temperatures of previous crystallization (see Table I) are indicated by the arrows.

to $x_{cL}(1 - x_{cL})$, while $A_c$ is proportional to $x_{cL}$ (see Discussion).

The corresponding results for the PEEK A sample crystallized at 302 and 272 °C are shown in Figure 6. One can observe three melting peaks in the DSC curve associated with three steps of increase in the long period. Two of these peaks (at 280 and 305 °C) are associated with a stepwise increase of $L$. The third one (from 320 to 348 °C) is correlated with two stepwise increases of $L$, separated by a region where $L$ stays constant. Again, the decrease of the crystallinity obtained by WAXS corresponds to the DSC results, while the decrease in $Q_{cor}$ is smaller than that of $A_c$ up to 320 °C.

The results for the PEEK B sample crystallized at six different temperatures are presented in Figure 7. Only three peaks in the DSC curve and two peaks in the $dA_c/dT$ curve can be distinguished, and the increase of $L$ becomes more or less continuous within the error of the experiment.

Finally, the results on PEKEKK crystallized at 352, 322, and 292 °C are represented in Figure 8. Three peaks can be clearly recognized in the DSC diagram. The long period again increases more or less continuously in the whole region of melting. While two of the DSC peaks agree well with the corresponding peaks in the $dA_c/dT$ curve, the middle one (at 352 °C) is shifted to 360 °C in the $dA_c/dT$ curve.

In both Figures 7 and 8, the decrease of $Q_{cor}$ is smaller than that of $A_c$ up to 320 °C.

## Discussion

**1. Comparison of DSC and WAXS Measurements.** While the DSC curves show clearly distinguishable peaks, the WAXS curves representing $A_c$ as a function of temperature do not show such obvious effects. This is due to the fact that the WAXS curves are equivalent to the integral of the DSC curves. However, it can be clearly recognized that each peak in the DSC curve corresponds to a change of the slope in the curve representing $A_c$.

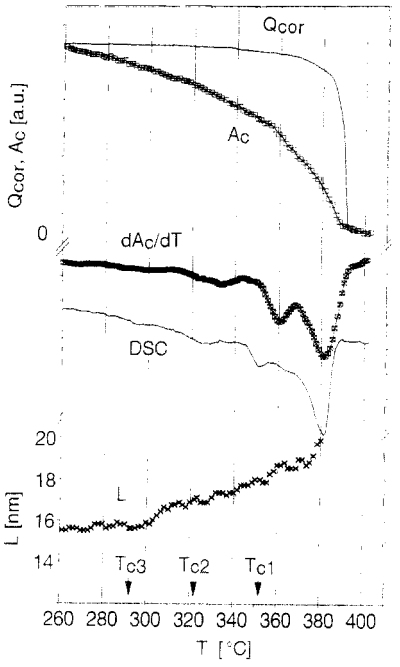


**Figure 8.** Corrected SAXS power $Q_{cor}$, integral intensity of the crystal reflections $A_c$, $A_c$ differentiated with respect to $T$, and long period $L$ as a function of temperature during heating (5 °C/min) of the PEKEKK sample. In addition, the DSC curve is also presented. The annealing temperatures of previous crystallization (see Table I) are indicated by the arrows.

For a better comparison with the DSC curves, in addition to $A_c$, $dA_c/dT$ has also been plotted. Due to the scattering of the WAXS data, as is usual when differentiating experimentally obtained curves, a smoothing procedure had to be applied to the WAXS curves before calculating the derivative of $A_c$ with respect to $T$. Applying different smoothing procedures resulted in essentially similar curves. From this we conclude that the smoothing does not falsify the $dA_c/dT$ curves.

The agreement between the DSC curves and the curves representing $dA_c/dT$ is quite satisfactory. The $dA_c/dT$ curves show (within differences which are smaller than 4 °C) peaks at the same temperature and of the same relative intensity as the corresponding DSC curves. There are only two exceptions: the DSC peak at 350 °C in Figure 8 which appears at 359 °C in the $dA_c/dT$ curve, and the DSC peak at 302 °C in Figure 7 which does not appear in the $dA_c/dT$ curve. These disparities may arise from the fact that any small scattering of the data of the $A_c$ curve leads to large effects in the differentiated curve $dA_c/dT$, which might not be eliminated by a smoothing procedure in all cases. Therefore the measurement of $A_c$ has been mainly used for comparison with the curve $Q_{cor}$.

A comparison of integrated DSC curves and the WAXS results obtained in this work was not possible because of two reasons: First, absolute measurements of the heat capacity were not performed in the DSC experiment and, therefore, the exact determination of the base line is not possible. Second, the Debye–Waller factor, which causes some decrease of $A_c$ with increasing temperature, was not determined.

**2. Comparison of SAXS and WAXS.** As pointed out in the Results section, the decrease in the corrected SAXS power $Q_{cor}$ with increasing temperature at temperatures up to about 40 °C below the melting point is smaller than the decrease of the intensity of the integrated WAXS crystal reflections $A_c$. By comparing the two curves, it is possible to obtain more information on structural changes during melting.[10,17-19] If the material is completely filled by spherulites, according to eq 1, one can write

$$Q = x_L x_{cL}(1 - x_{cL})(\Delta\rho)^2 \tag{5}$$

and the degree of crystallinity $x_c$, which is proportional to $A_c$, is given by

$$x_c = x_L x_{cL} \tag{6}$$

Now, if some lamellar stacks are melting, $x_L$ will decrease and both $Q$ and $A_c$ will decrease in proportion to $x_L$ and in proportion to each other. If, however, the degree of crystallinity within lamellar stacks decreases, for example, by melting of individual crystals (see next section), $x_{cL}$ will decrease. This will cause $x_c$ to become smaller in proportion to $x_{cL}$, while $Q$ will stay almost constant. For example, if $x_{cL}$ changes from 0.4 to 0.3, then $x_{cL}(1 - x_{cL})$ changes from 0.24 to 0.21. Considering this, we have to conclude that during melting in the region of lower temperatures a decrease of the degree of crystallinity within lamellar stacks occurs, rather than a melting of complete lamellar stacks.

Of course, some decrease of $A_c$ has to be attributed to the Debye–Waller factor. However, this factor is unable to explain the observed large disparity between the change of $Q_{cor}$ and $A_c$.

Errors might also result from the comparatively simple subtraction of the amorphous halo by means of a straight line. This possible error, too, will not effect our conclusion that the decrease of $A_c$ is larger than that of $Q_{cor}$ because of the following: First, the contribution of the amorphous halo is small compared to the disparity between $Q_{cor}$ and $A_c$ as shown in Figures 5–8. Second, the influence of the amorphous halo becomes larger with increasing temperature while $A_c$ decreases. Therefore, if at all, the influence of the amorphous halo would cause the disparity to seem smaller than is actually the case.

That partial melting occurs within the lamellar stacks was also concluded by Hsiao et al.[10] for PEEK and Gehrke et al.[17] as well as Bark et al.[18,19] for PET and PEN.

When the melting point is approached, the decrease of $Q$ becomes larger and $Q$ finally becomes zero at the melting point, as expected. The larger decrease can be explained by the fact that the product $x_{cL}(1 - x_{cL})$ becomes increasingly proportional to $x_{cL}$ as $x_{cL}$ decreases. In addition, complete lamellar stacks may disappear when the melting point is approached. To find out to what extent the second process takes place, a quantitative comparison of the change of $Q_{cor}$ and $A_c$ has to be performed. However, close to the melting point, this comparison would be questionable, because the long period becomes so large that it disappears within the primary beam, making an exact determination of the change of $Q$ impossible.

**3. Structural Changes during Partial Melting.** From the result that $Q_{cor}$ decreases less rapidly than $A_c$ it was concluded in the last section that the partial melting takes place within the lamellar stacks. Two possible models can be assumed for such a process:

(i) Single-crystal lamellae within the lamellar stacks which are thinner than neighboring lamellae are melting. The melting of one lamella would just double the local long period. However, because there exists a broad distribution of long periods and only a small fraction of lamellae are melting when the temperature is increased by a few degrees, one measures a gradual increase of the average long period rather than a doubling with increasing temperature.

Why are some crystal lamellae thinner than the other ones? We believe that in our experiment the thinner

lamellae are mainly formed during the crystallization at the lower temperatures $T_{c2}$, $T_{c3}$, etc. However, even in the case of exclusive isothermal crystallization, thinner lamellae may be formed at late stages of crystallization, i.e., during secondary crystallization.[10,29] These thinner lamellae may grow within regions where the space is restricted.

(ii) Due to entropy effects,[30-33] all crystal lamellae start to melt from their surfaces gradually with increasing temperature (surface melting). As a consequence of this process, the crystal thickness would decrease, the thickness of the amorphous region would increase, and the long period would stay constant.

Our results show that the long period generally increases with increasing temperature. When one assumes that individual thinner crystals lying between thicker crystals are melting, the increase in the long period should be especially pronounced where melting is largest, i.e., where the peaks in the DSC curves occur. According to our results this is generally the case. Therefore, it is obvious that the first effect plays a dominant role. It was also proved by other authors that thinner crystals are gradually melting with increasing temperature, for example, by Bassett et al.[9] and Lattimer et al.[12] using electron microscopy and by Hsiao et al.[10] using SAXS.

However, there also exist DSC peaks which do not correspond to an increase of the long period, for example, at 355 °C in Figure 5 and at 340 °C in Figure 6. From this we conclude that the second effect also takes place and is partly responsible for the decrease of crystallinity with increasing temperature. Such a surface melting was also considered by Lee and Porter[6] as an important effect during melting of PEEK.

**4. Is Partial Melting Followed by Recrystallization?** There also arises the question whether partial melting is followed by a recrystallization process leading to stacks of thicker lamellae showing a larger long period. A recrystallization of this type would also increase the average value of the long period. According to our previous investigations[13] and to other results reported in the literature,[3,9,10,14] we believe that this strongly depends on the thermal history of the sample.

First, let us consider a material crystallized at a relatively high temperature until it is completely filled by spherulites, and afterward slowly cooled either gradually or in steps. During the slow cooling some regions will crystallize which were not able to crystallize at the high temperature where the main crystallization took place. Two reasons may prevent crystallization at the high temperature:

1. *Spatial restriction*: Within the amorphous regions between the already existing lamellae there may be only enough space for the formation of comparatively thin lamellae, which are not stable at higher temperatures.

2. *Entropy effects*: Due to such effects, as mentioned in the previous section, the material close to the surfaces of the lamellae is able to crystallize only at temperatures considerably below the melting point.[30-33]

In both cases, when such a material is heated up after cooling these additional crystallized regions will melt when the temperature is increased, as discussed in the previous section, without being transformed into crystals again.

Such a behavior was first observed for PET, which was previously crystallized at 260 °C to the "end" of crystallization and cooled down slowly.[13] Though no further increase in crystallinity could be determined at 260 °C within hours, the crystallinity considerably increased during cooling. During heating, the crystallinity decreased again and no recrystallization took place. Furthermore, Cebe and Hong[8] have demonstrated for PEEK that a crystallization at high temperature "to the end" does not exclude the possibility that additional crystallization takes place during cooling. Wunderlich et al.[4] have shown that a crystallization at high temperature leads to a structure which allows the formation of additional crystals at lower temperatures but, at the same time, prevents these crystals from being as perfect as those formed at higher temperatures.

In the present investigation on the poly(aryl ether ketones) the material was first crystallized at a comparatively high temperature $T_{c1}$ and later on at lower temperatures. All melting peaks except the one at the highest temperature appeared below $T_{c1}$. Hence, we believe that recrystallization during heating does not take place. This is supported by the observation that no increase of crystallinity is observed by WAXS. Our conclusion that no recrystallization takes place is in agreement with results obtained by other authors.[10,11,14]

Second, we consider a material which was crystallized at a comparatively low temperature. In this case, in a subsequent heating of the sample up to the melting point, the effect of melting may be followed by recrystallization. The thinner crystals formed during crystallization at the lower temperature will melt and may then recrystallize being thicker and therefore thermally more stable. Of course, it depends on the rate of recrystallization compared to the heating rate whether or not recrystallization takes place.

Such a partial melting followed by recrystallization was observed in a PET sample previously crystallized at 140 °C.[13,17] Actually, by very fast heating, it was possible to melt a sample of PET already at 247 °C; this is 21 °C below the normal melting point. The melt existed only for a few seconds before recrystallization started. These results on PET are also supported by DSC measurements.[3] In addition, it has been demonstrated for PEEK that melting is followed by recrystallization if the previous crystallization of the poly(aryl ether ketones) occurs at a comparatively low temperature and the multiple melting peaks appear above this temperature.[5-7,25]

However, we have to point out that there also seems to exist a third situation. As was demonstrated by Bassett et al., double melting peaks may appear above the crystallization temperature, even without subsequent recrystallization. This was observed on a sample which was crystallized at a comparatively high temperature (310 °C). It was clearly shown by electron microscopy that lamellae of two different thicknesses existed. The lower melting point corresponded to the thin lamellae. Obviously, two lamellar populations of different thicknesses can grow even during isothermal crystallization, and no recrystallization occurs if only the population with thinner lamellae is melted.

In summary, we see that the situation is very complex. Therefore, we believe that it is correct for some authors to interpret the results by melting followed by recrystallization, while others assume that melting is not followed by recrystallization. As samples with different thermal histories are investigated, the processes which take place during heating will vary.

## Conclusions

Multiple melting peaks are observed by DSC during heating of poly(aryl ether ketones) which were previously crystallized at different temperatures $T_{c1} > T_{c2} > T_{c3}$ etc. by stepwise cooling from the melt. New insights into the structural changes during these melting processes are

obtained by comparing the changes of the degree of crystallinity $x_c$ with increasing temperature, as measured by DSC or WAXS, with the change of long period $L$ and scattering power $Q$ derived from SAXS. It is concluded that the multiple melting peaks arise from melting of crystals with different thicknesses which were formed during the crystallization at the temperatures $T_{c2}$, $T_{c3}$, etc. within already existing lamellar stacks. These stacks are built up by the thickest crystals grown at the highest crystallization temperatures $T_{c1}$.

In addition to the melting of single complete crystals, partial melting of the crystals, starting from their surfaces and caused by entropy effects, also seems to take place to some extent. It can be excluded that complete lamellar stacks are melting at temperatures where the additional melting peaks appear.

No recrystallization effects are observed after partial melting. However, from the discussion of the results from other investigations it is concluded that such recrystallization effects take place if the previous crystallization is performed at low temperatures.

The variation in the interpretation of multiple melting peaks in the literature (melting and recrystallization in contrast to different lamellar populations) is attributed to the fact that the structure and as a consequence the melting behavior are strongly affected by the thermal pretreatment, which varies in the different publications.

**Acknowledgment.** This work has been funded by the German Federal Minister for Research and Technology (BMFT) under Contract No. 05-5GUHXB. The authors thank Prof. J. C. Seferis for valuable information on the multiple melting peaks and intensive discussion. Furthermore, the authors are indebted to Dr. N. Everall (ICI), Mr. H. Müller (Hoechst), and Dr. H. Haberkorn (BASF) for kindly providing the investigated polymers.

## References and Notes

(1) Bell, J. P.; Murayama, T. J. *J. Polym. Sci.* **1969**, *7*, 1059.
(2) Roberts, R. C. *Polymer* **1969**, *10*, 117.
(3) Holdsworth, P. J.; Turner-Jones, A. *Polymer* **1971**, *12*, 195.
(4) Cheng, S. Z. D.; Cao, M.-Y.; Wunderlich, B. *Macromolecules* **1986**, *19*, 1868.
(5) Blundell, D. J. *Polymer* **1987**, *28*, 2248.
(6) Lee, Y.; Porter, R. S. *Macromolecules* **1987**, *20*, 1336.
(7) Lee, Y.; Porter, R. S.; Lin, J. S. *Macromolecules* **1989**, *22*, 1756.
(8) Cebe, P.; Hong, S.-D. *Polymer* **1986**, *27*, 1183.
(9) Bassett, D. C.; Olley, R. H.; Raheil, I. A. M. *Polymer* **1988**, *29*, 1745.
(10) Hsiao, B. S.; Gardner, K. H.; Wu, D. Q.; Liang, B.; Chu, B. *Polym. Prepr. (Am. Chem. Soc., Div. Polym. Chem.)* **1992**, *33*, 265.
(11) Könnecke, K. *Angew. Makromol. Chem.* **1992**, *198*, 15.
(12) Lattimer, M. P.; Hobbs, J. K.; Hill, M. J.; Barham, P. J. *Polymer* **1992**, *33*, 3971.
(13) Zachmann, H. G.; Stuart, H. A. *Makromol. Chem.* **1960**, *41*, 148.
(14) Chang, S.-S. *Polym. Commun.* **1988**, *29*, 138.
(15) Copeland, S. D. MS Thesis, University of Washington, Seattle, 1989.
(16) Copeland, S. D.; Seferis, J. C., to be published.
(17) Gehrke, R.; Riekel, C.; Zachmann, H. G. *Polymer* **1989**, *30*, 1582.
(18) Bark, M.; Zachmann, H. G. *Acta Polym.*, submitted.
(19) Bark, M.; Schulze, C.; Zachmann, H. G. *Polym. Prepr. (Am. Chem. Soc., Div. Polym. Chem.)* **1990**, *31*, 106.
(20) Elsner, G.; Riekel, C.; Zachmann, H. G. *Adv. Polym. Sci.* **1985**, *67*, 1.
(21) Kortleve, G.; Vonk, C. G. *Kolloid Z.* **1968**, *225*, 124.
(22) Vonk, C. G.; Kortleve, G. *Kolloid Z.* **1967**, *220*, 19.
(23) Zachmann, H. G.; Wutz, C. *Polym. Prepr. (Am. Chem. Soc., Div. Polym. Chem.)* **1992**, *33*, 261.
(24) Fischer, E. W.; Kloos, F.; Lieser, G. *Polym. Lett.* **1969**, *7*, 845.
(25) Blundell, D. J.; Osborn, B. N. *Polymer* **1983**, *24*, 953.
(26) Hoechst, Hostatec product information, Frankfurt, Feb 1991.
(27) BASF, High Heat Resistant Thermoplastics, Ludwigshafen, 1991.
(28) Schermann, W.; Zachmann, H. G. *Kolloid Z. Z. Polym.* **1990**, *241*, 921.
(29) Zachmann, H. G.; Wutz, C. In *Nato ASI Ser.*, in press.
(30) Zachmann, H. G. *Kolloid Z. Z. Polym.* **1967**, *216*, 180.
(31) Zachmann, H. G.; Peterlin, A. *J. Macromol. Sci.* **1969**, *B3*, 495.
(32) Ewers, H. M.; Zachmann, H. G.; Peterlin, A. *J. Macromol. Sci.* **1972**, *B6*, 695.
(33) Fischer, E. W. *Kolloid Z. Z. Polym.* **1967**, *218*, 97.